2009 American Control Conference
Hyatt Regency Riverfront, St. Louis, MO, USA
June 10-12, 2009

Nonlinear Control Design for an Air-breathing Engine with State Estimation

J. Rajasekaran, A. Maity, A. Lal and R. Padhi

Abstract— **A nonlinear control design approach is presented in this paper for a challenging application problem of ensuring robust performance of an air-breathing engine operating at supersonic speed. The primary objective of control design is to ensure that the engine produces the required thrust that tracks the commanded thrust as closely as possible by appropriate regulation of the fuel flow rate. However, since the engine operates in the supersonic range, an important secondary objective is to ensure an optimal location of the shock in the intake for maximum pressure recovery with a sufficient margin. This is manipulated by varying the throat area of the nozzle. The nonlinear dynamic inversion technique has been successfully used to achieve both of the above objectives. In this problem, since the process is faster than the actuators, independent control designs have also been carried out for the actuators as well to assure the satisfactory performance of the system. Moreover, an extended Kalman Filter based state estimation design has been carried out both to filter out the process and sensor noises as well as to make the control design operate based on output feedback. Promising simulation results indicate that the proposed control design approach is quite successful in obtaining robust performance of the air-breathing system.**

Index Terms- Air-breathing engine, Combustion system, Dynamic Inversion, Extended Kalman Filter (EKF).

I. INTRODUCTION

The objective of this paper is to present a modern system theory based nonlinear control design for successful operation of an air-breathing engine operating at supersonic speed (see Fig. 1). The primary objective of the control design of such an air-breathing engine is to ensure that the engine dynamically produces the thrust that tracks a commanded value of thrust as closely as possible by regulating the fuel flow to the combustion system. This is done by regulating the signal to the Fuel Supply System (FSS) which then injects the desired quantum of fuel into the combustion chamber.

Since the engine operates in the supersonic range, a critical constraint of the problem is to manage the shock configuration in the intake section of the engine as much forward as possible such that maximum pressure recovery is achieved, which leads to minimum fuel requirement. However, it should also be assured that the shock does not travel outside the intake section at any point of time since it is extremely difficult to bring it back into the intake once it goes out. It has been observed that whereas the thrust produced can be manipulated primarily by varying the fuel flow rate, the primary mechanism of controlling the shock location is by manipulating the intake back pressure, which in turn can be manipulated by varying the nozzle throat area [1]. However, note that both the control variables do affect both the thrust produced as well as the back pressure through complex inter coupling. As obvious from the discussion above, the problem that needs to be addressed basically involves tracking of the thrust command and regulation of the back pressure. Even though the linear PID design followed by gain scheduling has been attempted to address this problem recently [2], the main objective of this paper is to present a modern system theory based effective nonlinear control design approach without approximating the system dynamics. Perhaps an obvious choice in this regard is the technique of dynamic inversion [3], which has been used in this paper. Dynamic inversion offers several advantages that include: (i) guaranteed asymptotic tracking of the output signal, (ii) avoidance of the exhaustive gain scheduling process, (iii) generic nature of the design, where future design changes and/or model improvements can easily be accommodated and (iv) closed form nature of the solution (and hence, no computational complexity issues).

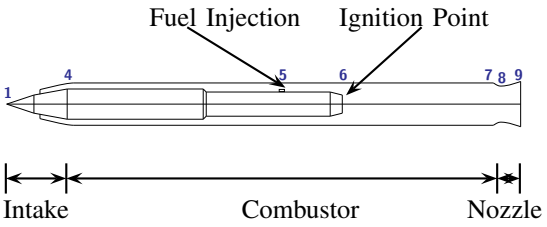

Fig. 1. Schematic of a typical supersonic air-breathing engine

One important requirement for any control design is to be practically feasible for implementation is to obtain satisfactory results after incorporating the actuator dynamics. In the case of the air-breathing engine the actuators used are the throat area actuator and fuel supply system (FSS), which are relatively quite slower than the process itself. Because of this reason, separate controllers for the actuators have been designed as well (using the dynamic inversion technique).

A drawback of any state feedback design (dynamic inversion included) is the need to obtain the state information. However, all of state variables are seldom directly mea-

This work was not supported by any organization

J. Rajasekaran, Former project assistant, was in the Dept. of Aerospace Engineering, Indian Institute of Science, Bangalore, India.

A. Maity, Ph.D. Student, is in the Dept. of Aerospace Engineering, Indian Institute of Science, Bangalore, India.

A. Lal, Former consultant, was in Coral Digital Technologies, Bangalore, India.

R. Padhi (Contact Author) is an Asst. Professor in the Dept. of Aerospace Engineering, Indian Institute of Science, Bangalore, India. Tel. +91-80-2293-2756, padhi@aero.iisc.ernet.in

surable. Moreover, the measured variables are corrupted by the sensor noise and the system dynamics is influenced by process noise as well. Hence, there is a need to estimate the system states both to filter out the noises as well as to make available the numerical values of the states (with as minimum error as possible) for control computation. To meet these requirements, an Extended Kalman Filter [4] based state estimation design has been carried out in parallel to augment the proposed control design. Here, it is proposed to use only two sensors, one for measuring the intake back pressure and the other for measuring the temperature at the nozzle throat. Additional sensor requirements are eliminated by bringing in appropriate assumptions and intelligent manipulation of the expressions, which do not lead to deterioration in the performance of the feedback system.

The overall control design strategy has been successfully tested for one suggested operating points for two different tracking signals. Extensive simulation studies have been carried out to test the performance and stability of the closed-loop system. Promising simulation results indicate that the proposed control design approach is quite successful in obtaining robust performance of the air-breathing system, both for tracking the thrust command as well as to maintain the back pressure in the intake at a desired value that is close to its upper critical value (with sufficient margin for robustness).

II. CONTROL DESIGN USING DI

In this section, the basic idea of the control design is presented, assuming ideal conditions such as all state information being available for feedback, availability of infinite bandwidth actuators etc.

The air-breathing combustion system, shown in Fig. 1 [1], consists of various components, marked as various stations. The intake model is obtained from CFD, whereas a quasi-1D code represents the fluid mechanics and the reaction mechanisms for the combustor model. The nozzle is modeled as a simple isentropic component. The system dynamics for the combustion system are given by the following set of coupled nonlinear differential equations

$$\dot{P}_4 = \frac{1}{\tau_{54}}\left(P_{4ss} - P_4\right) \tag{1}$$

$$\dot{P}_5 = \frac{1}{\tau_{75}}\left(P_{5ss} - P_5\right) \tag{2}$$

$$\dot{T}_{05} = \frac{1}{\tau_{45}}\left(T_{05ss} - T_{05}\right) \tag{3}$$

$$\ddot{m}_5 = \frac{1}{\tau_{45}}\left(\dot{m}_{5ss} - \dot{m}_5\right) \tag{4}$$

$$\dot{P}_7 = \frac{1}{B}\left[\dot{m}_7 - A_{th}\frac{r_n P_{07}\sqrt{\gamma}}{\sqrt{RT_{07}}}\left(\frac{2}{\gamma+1}\right)^{\frac{\gamma+1}{2(\gamma-1)}}\right] \tag{5}$$

$$\dot{P}_{07} = \frac{1}{\tau_{57}}\left(P_{7ss} - P_{07}\right) \tag{6}$$

$$\dot{T}_{07} = \frac{1}{\tau_{57}}\left(T_{07ss} - T_{07}\right) \tag{7}$$

$$\ddot{m}_7 = \frac{1}{\tau_{57}}\left(\dot{m}_{7ss} - \dot{m}_7\right) \tag{8}$$

where, P_i is pressure at station i, P_{0i} and T_{0i} are stagnation pressure and temperature at station i respectively, $\dot{m}_i$ is the mass flow rate at station i, τ_{ij} is the time constant between stations i (1 to 9) and j (1 to 9), B is the back pressure factor, R is the universal gas constant and A_{th} is the throat area control.

The system output is the thrust T which is given by

$$\begin{aligned} T &= \left(\frac{r_n P_{07}}{\left[1+\frac{\gamma-1}{2}M_9^2\right]^{\gamma/(\gamma-1)}} - P_1\right)A_9 \\ &\quad + A_{th}\frac{\gamma r_n P_{07} M_9}{\sqrt{1+\frac{\gamma-1}{2}M_9^2}}\left(\frac{2}{\gamma+1}\right)^{\frac{\gamma+1}{2(\gamma-1)}} \\ &\quad - \dot{m}_4 M_1\sqrt{\gamma' R T_1} \\ &= f\left(P_{07}, M_9\left(A_{th}\right), A_{th}, \dot{m}_4\right) \end{aligned} \tag{9}$$

where, γ and γ' are the ratio of specific heats for the combustor exhausted mixture (taken as 1.2) and free stream air (taken as 1.4) respectively, M_1 and M_9 are the mach numbers at stations 1 and 9 respectively, T_1 is the temperature at station 1, $\dot{m}_4$ is the mass flow rate at station 4, r_n is the recovery factor across the nozzle, P_1 is the static pressure at station 1, A_9 is the nozzle exit area.

In (1)-(8), the subscript 'ss' means steady state terms in the state equations, which are computed by linear interpolating within the set of data estimated using computational fluid dynamics (CFD). The functional relation for the steady state terms are given as [2]

$$\left[P_{4ss}, T_{05ss}, \dot{m}_{5ss}, \tau_{45}, \tau_{54}\right] = f_1\left(\dot{m}_4, T_{04}, P_5\right) \tag{10}$$

$$\begin{aligned} &\left[P_{5ss}, T_{07ss}, P_{07ss}, \dot{m}_{7ss}, \tau_{57}, \tau_{75}, B, Tpk\right] \\ &\qquad = f_2\left(\dot{m}_5, \dot{m}_f, T_{05}, P_7\right) \end{aligned} \tag{11}$$

For interpolation we have used the Delaunay-based triangulation method [5]. For more details of the model one can refer to [1], [2].

A. Objectives of Control Design and Control Allocation Philosophy:

The primary objective of the control design is to ensure that the engine tracks the commanded value of thrust. However, since the engine operates in the supersonic range, it is important to maintain the shock configuration in the intake section of the engine, which depends on pressure P_4 at station 4 of the engine for a given flight condition (altitude, Mach number and angle of attack), such that a high-air inflow rate is achieved. If the pressure P_4 exceeds a 'critical value' P_{4C} (this value is known to us from CFD simulation results) then the air flow rate into the engine is reduced drastically. This is catastrophic for engine operation. On other hand, the low values of P_4 deteriorate the pressure recovery across the intake section, which is also not desirable as it necessitates more fuel addition in the combustor to add enough energy to the air within the engine to obtain the required thrust. If

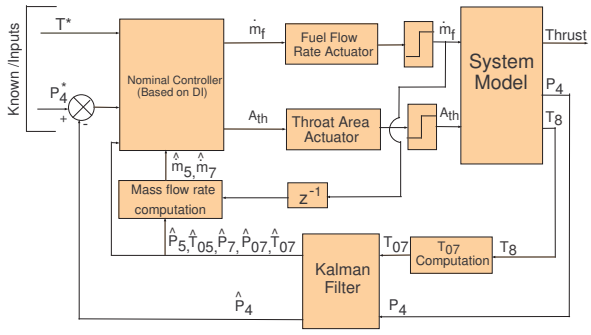

Fig. 2. Block diagram for feedback control of the air breathing engine

pressure recovery is high, a lot of the available energy of the free stream air is conserved and consequently, less fuel is required in the combustor to obtain the desired thrust. Consequently, to get high pressure recovery, the second objective of the control design is chosen: to ensure that the pressure P_4 is held fixed at a predefined value P_{4opt} which is marginally less than P_{4C} ($P_4 < P_{4C}$); the small gap (P_{4C} - P_{4opt}) is left to account for the fluctuations in the flight conditions and the system noise that will affect P_4.

The basic philosophy of this state feedback nonlinear control design is summarized in the block diagram in Fig. 2.

B. Throat Area Control Design:

As mentioned in Section B, the objective of the throat area controller is to maintain P_4 at an optimum value $P_{4_{opt}}$. In the subsequent discussion in this paper, the upper critical limit (P_{4C}) of P_4 is referred to as $P_{4_{max}}$, whereas the lower critical limit of P_4 is $P_{4_{min}}$. The $P_{4_{opt}}$ value is calculated for various flight conditions like Mach, altitude and angle of attack by taking different percentage value of difference between $P_{4_{max}}$ and $P_{4_{min}}$ below $P_{4_{max}}$.

First, the error between the terms P_4 and $P_{4_{opt}}$ is defined as,

$$E_{P_4} \triangleq P_4 - P_{4_{opt}} \tag{12}$$

The error term is differentiated until the control term (A_{th}) appears and we get following expression,

$$\dddot{E}_{P_4} = f_{P_4} + g_{P_4} A_{th} \tag{13}$$

Now the A_{th} expression is

$$A_{th} = -\frac{1}{g_{P_4}} \left[f_{P_4} + k_2 \ddot{E}_{P_4} + k_1 \dot{E}_{P_4} + k_0 E_{P_4} \right] \tag{14}$$

where constants k_0, k_1 and k_2 are the design. Using the expression derived in (14) the A_{th} control is computed for P_4 to track $P_{4_{opt}}$.

C. Fuel Flow Rate Control Design:

The fuel flow rate controller is designed by assuming an asymptotic expression. The asymptotic condition is attained when P_4 approaches $P_{4_{opt}}$, that is, the error terms and their derivatives, $\dddot{E}_{P_4}$, $\ddot{E}_{P_4}$, $\dot{E}_{P_4}$, E_{P_4} become zero. Proceeding with the above assumptions a reduced form for the A_{th} can be written as, $A_{th} = -\frac{f_{P4}}{g_{P_4}}$. From this assumption also we can write, $P_4 = P_{4opt}$, $\dot{P}_4 = 0$, $\dot{P}_5 = 0$. The final reduced relation obtained for A_{th} is given below,

$$A_{th} = \frac{\frac{\partial P_{5ss}}{\partial T_{05}} \left[\frac{B}{\tau_{45}} \left(T_{05ss} - T_{05} \right) \right] + \frac{\partial P_{5ss}}{\partial P_7} \dot{m}_7}{\frac{r_n P_{07} \sqrt{\gamma}}{\sqrt{R T_{07}}} \left(\frac{2}{\gamma+1} \right)^{\frac{\gamma+1}{2(\gamma-1)}} \frac{\partial P_{5ss}}{\partial P_7}} \tag{15}$$

From (15) we compute the P_{07} expression and put this P_{07} expression in (9). We get the following thrust expression,

$$\begin{aligned} T \;=\; & \left[\left(\frac{\frac{\partial P_{5ss}}{\partial T_{05}} \left[\frac{1}{\tau_{45}} \left(T_{05ss} - T_{05} \right) \right] B}{\frac{\partial P_{5ss}}{\partial P_7}} + \dot{m}_7 \right) \frac{\sqrt{T_{07}}}{\beta} \right] \\ & \times \left[\frac{C_T^1}{A_{th}} A_9 + C_T^2 \right] + \left[-P_1 A_9 - C_T^3 \right] \end{aligned} \tag{16}$$

where, $C_T^1 \triangleq \frac{1}{\left[1 + \frac{\gamma-1}{2} M_9^2\right]^{\frac{\gamma}{\gamma-1}}}$,
$C_T^2 \triangleq \frac{\gamma M_9}{\sqrt{1 + \frac{\gamma-1}{2} M_9^2}} \left(\frac{2}{\gamma+1} \right)^{\frac{\gamma+1}{2(\gamma-1)}}$, $C_T^3 \triangleq \dot{m}_4 M_1 \sqrt{\gamma' R T_1}$.
The fuel mass flow rate controller is also designed using the dynamic inversion technique and the error term is defined as

$$E_T = T - T^* \tag{17}$$

Next, following the principle of dynamic inversion, the following error dynamic is enforced to synthesize the $\dot{m}_f$ controller.

$$\dot{E}_T + k_T E_T = 0 \tag{18}$$

where, k_T is the control design gain. Using the expression for T in (9) and carrying out the necessary algebra, one can derive the expression for $\dot{m}_f$. However, there is a small problem in directly attempting to solve for the $\dot{m}_f$. This is because of the fact that in the interpolation function (11) $\dot{m}_f$ is an input variable and it is not available before solving for this control term. To circumvent this problem, we have first expressed $\dot{m}_f$ as

$$\dot{m}_f = \dot{m}_{f_i} + \Delta \dot{m}_f \tag{19}$$

where $\dot{m}_{f_i}$ is the previous fuel flow rate control value, which is assumed to be known. The $\Delta \dot{m}_f$ term then acts as the incremental control variable, which is treated as the unknown quantity. The interpolation is carried out with respect to the $\dot{m}_{f_i}$, whereas the true value of the control is given by (19). This algebra is possible with the assumption that $\Delta \dot{m}_f$ is small and hence it is not supposed to introduce any error in the interpolated values in (11). Note that the derivative terms (which are critical for control design) will remain same as long as the updated value remains within the same interpolation domain, since the interpolation function is linear.

The thrust derivative term can be given as

$$\begin{aligned}\dot{T} &= \frac{\partial T}{\partial T_{07}}\dot{T}_{07} + \frac{\partial T}{\partial T_{05}}\dot{T}_{05} \\ &= \frac{\partial T}{\partial T_{07}}\left(\frac{1}{\tau_{57_i} + \frac{\partial \tau_{57}}{\partial \dot{m}_f}\Delta\dot{m}_f}\right) \\ &\quad \times\left(T_{07ss_i} + \frac{\partial T_{07ss}}{\partial \dot{m}_f}\Delta\dot{m}_f - T_{07}\right) + F_T \quad (20)\end{aligned}$$

where, $F_T = \frac{\partial T}{\partial T_{05}}\left[\frac{1}{\tau_{45}}\left(T_{05ss} - T_{05}\right)\right]$

Finally we get the following equation,

$$\begin{aligned}\Delta\dot{m}_f = &\frac{\tau_{57}\left[\dot{T}^* - k_T\left(T - T^*\right) - F_T\right]}{\frac{\partial T}{\partial T_{07}}\frac{\partial T_{07ss}}{\partial \dot{m}_f} - \frac{\partial \tau_{57}}{\partial \dot{m}_f}\left[\dot{T}^* - k_T\left(T - T^*\right) - F_T\right]} \\ &- \frac{\frac{\partial T}{\partial T_{07}}\left[T_{07ss} - T_{07}\right]}{\frac{\partial T}{\partial T_{07}}\frac{\partial T_{07ss}}{\partial \dot{m}_f} - \frac{\partial \tau_{57}}{\partial \dot{m}_f}\left[\dot{T}^* - k_T\left(T - T^*\right) - F_T\right]} \quad (21)\end{aligned}$$

where, $k_T > 0$ is the control design gain. We get the updated $\dot{m}_f$ using the (21) in (19).

III. INCORPORATION OF ACTUATOR DYNAMICS

As pointed out in Section I, we have designed the separate controllers for both the throat area actuator as well as the FSS system for the validation of the control design, and this is discussed in this section.

A. Control Design for Throat Area Actuator

The throat area actuator acts as a tool to maintain the throat of the supersonic nozzle in an appropriate dimension. The throat dimension is varied to control the inlet pressure of the engine. The state-space form of the throat area actuator dynamics is given by

$$\begin{bmatrix} \dot{A}_{th} \\ \ddot{A}_{th} \end{bmatrix} = \begin{bmatrix} 0 & 1 \\ -a_1 & -a_2 \end{bmatrix}\begin{bmatrix} A_{th} \\ \dot{A}_{th} \end{bmatrix} + \begin{bmatrix} 0 \\ a_1 \end{bmatrix} Act_{inp} \quad (22)$$

where, a_1 and a_2 are constants, Act_{inp} is the control input provided to the throat area actuator, and A_{th} is the system output. For designing the controller for the throat area actuator we have used the dynamic inversion technique. The goal of the controller design is: $A_{th} \rightarrow A^*_{th}$ as soon as possible, where A^*_{th} is the commanded value of A_{th}. So the error is $E_{th} = A_{th} - A^*_{th}$. Here the relative degree between Act_{inp} and A_{th} is two and we get the following expression

$$\begin{aligned}Act_{inp} &= \frac{\ddot{A}^*_{th} + a_1 A_{th} + a_2 \dot{A}_{th}}{a_1} \\ &\quad - \frac{\left[k_{a_1}(\dot{A}_{th} - \dot{A}^*_{th}) + k_{a_0}(A_{th} - A^*_{th})\right]}{a_1} \quad (23)\end{aligned}$$

where, k_{a_0} and k_{a_1} are design constants. Note that we have assumed that $\dot{A}^*_{th} = 0$ and $\ddot{A}^*_{th} = 0$ because information about the derivatives of A^*_{th} is typically not available in practice.

Here the throat area actuator is assumed to have a geometrical limit of $\pm 12\%$ from the nominal throat area of $0.0335\mathrm{m}^2$ imposed in the actuator output.

B. Control Design for Fuel Supply System

The function of FSS is to maintain the pressure within the actuator and as well as provide the system with the required fuel flow rate demanded by the controller [2].

IV. EXTENDED KALMAN FILTER:

A. Implementation of Extended Kalman Filter:

Let the system can be described by the nonlinear dynamic state space model

$$\dot{\mathbf{x}}(t) = f\left[\mathbf{x}(t), \mathbf{u}(t)\right] + G\mathbf{w}(t) \quad (24)$$

where, $\mathbf{x}(t_0)$ is the initial state vector, $\mathbf{w}(t)$ is zero mean Gaussian white noise. Let the available discrete-time output be modeled as

$$\mathbf{y}_k = h\left(\mathbf{x}_k\right) + \mathbf{v}_k \quad (25)$$

$$\dot{\hat{\mathbf{x}}}(t) = f\left[\hat{\mathbf{x}}(t), \mathbf{u}(t)\right] \quad (26)$$

which is propagated for predicting the future states until the new measurement comes. With measurement information the states are corrected and error covariance matrix is also updated. For more details of EKF, one can refer to [4].

B. Disturbance models:

One major source of disturbance in the combustion system is due to heat release fluctuations in the combustion chamber which drives the chamber acoustics. This is called as 'bulk mode' as the combustion chamber of the air-breathing combustion system, with the choked nozzle, behaves like a single bulk volume [6]. This phenomenon is modeled using a second-order transfer function with a frequency of 30 Hz and an estimated damping ratio of 0.1 and is given by

$$\frac{w_1(t)}{n_1(t)} = \frac{35531}{s^2 + 37.7s + 35531} \quad (27)$$

The other major source of disturbance is due to turbulent fluctuations in the intake diffuser and the combustor [7], which is taken to be broadband noise and modeled as a low-pass filter with the break frequency of 100 Hz. The transfer function of this model is given by,

$$\frac{w_2(t)}{n_2(t)} = \frac{394800}{s^2 + 754s + 394800} \quad (28)$$

Both disturbance models are exited by a Gaussian random functions with zero means and $\left(0.0002 \times P_4(0)\right)^2$ and $\left(0.00006 \times P_4(0)\right)^2$ variances respectively. Here $n_1(t)$, $n_2(t)$ are the white noises and $w_1(t)$, $w_2(t)$ are the colored noises. Note that the perturbation due to turbulent fluctuations never exceeds 1% of P_4 at all frequencies, and the perturbation due to the bulk mode never exceeds 5% at the resonant Helmholtz frequency of 30 Hz.

We represent the transfer function of the first disturbance model (27) in the following observable canonical form

$$\dot{\mathbf{x}}_{w_1} = \begin{bmatrix} \dot{x}_{w_{11}} \\ \dot{x}_{w_{12}} \end{bmatrix} = A_{w_1}\mathbf{x}_{w_1} + B_{w_1}n_1 \quad (29)$$

$$w_1 = C_{w_1}\mathbf{x}_{w_1} + D_{w_1}n_1 \quad (30)$$

where, $\mathbf{x}_{w_1} = \begin{bmatrix} x_{w_{11}} & x_{w_{12}} \end{bmatrix}^T$ is the state vector of the first shaping filter [8]. Similarly, we represent the transfer function of the second disturbance model (28) in the following observable canonical form,

$$\dot{\mathbf{x}}_{w_2} = \begin{bmatrix} \dot{x}_{w_{21}} \\ \dot{x}_{w_{22}} \end{bmatrix} = A_{w_2}\mathbf{x}_{w_2} + B_{w_2}n_2 \tag{31}$$

$$w_2 = C_{w_2}\mathbf{x}_{w_2} + D_{w_2}n_2 \tag{32}$$

where, $\mathbf{x}_{w_2} = \begin{bmatrix} x_{w_{21}} & x_{w_{22}} \end{bmatrix}^T$ is the state vector of the second shaping filter.

C. The augmented actual system dynamics:

The state space representation of augmented actual system dynamics is given below

$$\dot{\mathbf{x}}_{aug} = \begin{bmatrix} \dot{\mathbf{x}} \\ \dot{\mathbf{x}}_w \end{bmatrix} = \begin{bmatrix} f(\mathbf{x},\mathbf{u}) & GC_w\mathbf{x}_w \\ 0 & A_w\mathbf{x}_w \end{bmatrix} + \begin{bmatrix} GD_w \\ B_w \end{bmatrix}\mathbf{n} \tag{33}$$

$$\mathbf{y}_{aug} = \begin{bmatrix} H & 0 \end{bmatrix}\begin{bmatrix} \mathbf{x} \\ \mathbf{x}_w \end{bmatrix} + \mathbf{v} \tag{34}$$

where, $\mathbf{x} = \begin{bmatrix} P_4 & P_5 & T_{05} & P_7 & P_{07} & T_{07} \end{bmatrix}^T$;
$\mathbf{x}_w = \begin{bmatrix} x_{w_{11}} & x_{w_{12}} & x_{w_{21}} & x_{w_{22}} \end{bmatrix}^T$; $\mathbf{n} = \begin{bmatrix} n_1 & n_2 \end{bmatrix}^T$;
$\mathbf{v} = \begin{bmatrix} v_1 & v_2 \end{bmatrix}^T$; $A_w = \begin{bmatrix} A_{w_1} & 0 \\ 0 & A_{w_2} \end{bmatrix}$;
$B_w = \begin{bmatrix} B_{w_1} & 0 \\ 0 & B_{w_2} \end{bmatrix}$; $C_w = \begin{bmatrix} C_{w_1} & 0 \\ 0 & C_{w_2} \end{bmatrix}$;
$D_w = \begin{bmatrix} D_{w_1} & 0 \\ 0 & D_{w_2} \end{bmatrix}$;
$G = \begin{bmatrix} -1/\tau_{54} & 0 & 0 & 0 & 0 & 0 \\ -1/\tau_{54} & 0 & 0 & 0 & 0 & 0 \end{bmatrix}^T$;
$H = \left[\frac{\partial h}{\partial x}\right]_{\hat{x}_k} = \begin{bmatrix} 1 & 0 & 0 & 0 & 0 & 0 \\ 0 & 0 & 0 & 0 & 0 & \frac{1}{(1+(\gamma-1)/2)} \end{bmatrix}$

In this problem, the measurable outputs assumed P_4 and T_{07} are [9]. This assumption is justified from the fact that,

$$T_{07} = T_{08} = T_8\left(1 + (\gamma-1)/2\right) \tag{35}$$

In this problem only $P_4,\ P_5,\ T_{05},\ P_7, P_{07}$ and T_{07} are estimated. Here we have assumed that the variations of $\ddot{m}_5$ and $\ddot{m}_7$ are small and introduce the assumption that $\ddot{m}_5$=$\ddot{m}_7 = 0$. Because of this assumption, it is clear from the system dynamics that (see (4) and (8)) $\dot{m}_5 = \dot{m}_{5_{ss}}$ and $\dot{m}_7 = \dot{m}_{7_{ss}}$, where $\dot{m}_{5_{ss}}$ and $\dot{m}_{7_{ss}}$ are evaluated from the estimated states using the interpolation functions provided as part of the system modeling. The above procedure was introduced to minimize the number of sensors required.

D. The augmented estimated system dynamics:

The state space representation of augmented estimated system dynamics is given below,

$$\dot{\hat{\mathbf{x}}}_{aug} = \begin{bmatrix} \dot{\hat{\mathbf{x}}} \\ \dot{\hat{\mathbf{x}}}_w \end{bmatrix} = \begin{bmatrix} f(\hat{\mathbf{x}},\mathbf{u}) & GC_w\hat{\mathbf{x}}_w \\ 0 & A_w\hat{\mathbf{x}}_w \end{bmatrix} \tag{36}$$

$$\hat{\mathbf{y}}_{aug} = \begin{bmatrix} H & 0 \end{bmatrix}\begin{bmatrix} \hat{x} \\ \hat{x}_w \end{bmatrix} \tag{37}$$

where, $\hat{\mathbf{x}} = \begin{bmatrix} \hat{P}_4 & \hat{P}_5 & \hat{T}_{05} & \hat{P}_7 & \hat{P}_{07} & \hat{T}_{07} \end{bmatrix}^T$ and $\hat{\mathbf{x}}_w = \begin{bmatrix} \hat{x}_{w_{11}} & \hat{x}_{w_{12}} & \hat{x}_{w_{21}} & \hat{x}_{w_{22}} \end{bmatrix}^T$.

TABLE I
SELECTION OF SAMPLING TIME STEPS AND GAINS

Loop	Time step (msec)	Settling time (sec)	Gain
Throat area control	2	Settling time = 0.05, Overshoot = 5%, Third pole location = -240	400, 5.184×10^4 and 3.225×10^6
Fuel flow rate control	2	0.25	16
Throat area Actuator	0.2	Settling time = 0.01, Overshoot = 5%	800 and 3.36×10^5
FSS Actuator	0.2	0.01	400

E. Design parameters selection:

The covariance matrices selection has been done following some 'standard guidelines' [4], as well as intensive technical discussion with experts in this field. The measurement noise covariance matrix has finally been selected as $R = \mathrm{diag}\left(\left(0.02 \times P_4(0)\right)^2, \left(0.02 \times T_8(0)\right)^2\right)$
The initial error covariance matrix P_0 and the process noise covariance matrix Q have been selected depended upon the operating points. The process noise covariance matrix Q serves as the 'tuning parameter', which is varied until the filter converges and satisfactory performance is obtained.

EKF usually produce highly fluctuating outputs initially. It takes some time before the computed matrix and the associated Kalman gain stabilizes. This filter stabilization duration is taken as 0.2 Sec., during which the system operates in open loop (with initial control values being held constant).

V. RESULTS AND DISCUSSION

In this section, system performance with actuator dynamic and EKF is shown at various possible operating points and with respect to some standard test signals. The selection of sampling time steps and gains for the throat area controller, fuel flow rate controller, throat area actuator and FSS actuator are given in Table I.

A. Operating point: Mach number = 2.1, AoA = 0° and Altitude = 1.4km

In this simulation study, the initial conditions of states are selected around the expected operating point given by the flight condition of 2.1 Mach number, 0°AoA and 1.4km altitude with initial throat area control value $A_{th} = 0.0355\mathrm{m}^2$. The P_4 value is commanded to $P_{4_{opt}} = 5.19 \times 10^5\mathrm{Pa}$. The tracking signals for the commanded thrust with amplitude $9880N \pm 400N$ are provided as a square wave in Fig. 3 and Fig. 4 and a sine wave in Fig. 5. Here we have selected the initial error covariance matrix $P_0 = \mathrm{diag}\left(10^{10}, 10^{10}, 10^4, 10^{10}, 10^{10}, 10^4, 10^8, 10^8,\ 10^8, 10^8\right)$ and also after a lot of simulation study we have finally put down the process noise covariance matrix $Q = I_2$. In Fig. 3 and Fig. 5, the estimated thrust tracks the commanded

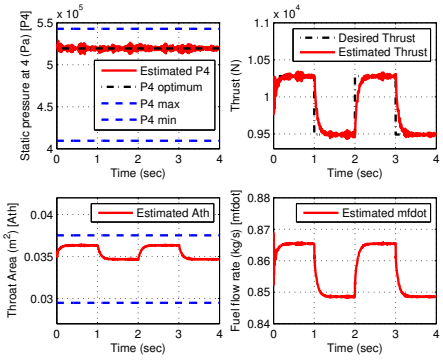

Fig. 3. P_4, thrust and controllers responses at 2.1 Mach

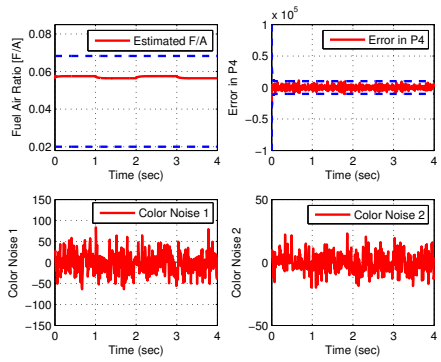

Fig. 4. F/A, Error in P_4 and color noises responses at 2.1 Mach

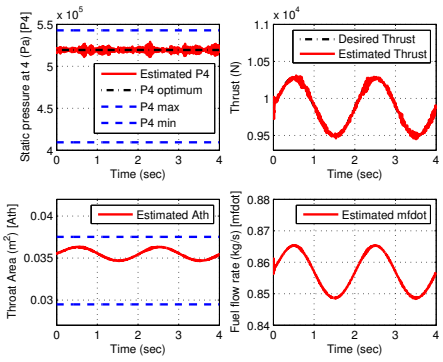

Fig. 5. P_4, thrust and controllers responses at 2.1 Mach

thrust well and the trajectory of the fuel flow rate controller is shown. In these Figures, the estimated P_4 tracks the $P_{4_{opt}}$ extremely well and remains within the prescribed bounds and also the performance of the estimated throat area controller remains within the maximum and minimum limits. Figure 4 clearly shows that the F/A ratio remains well within the prescribed bounds; the error between the measured P_4 and estimated P_4 remains within the 3σ bounds and the corresponding color noise outputs of these shaping filters are shown. The same color noise outputs, shown in Fig. 4, are used for sine wave commanded thrust tracking.

VI. CONCLUSIONS

The nonlinear dynamic inversion technique has been successfully used to synthesize an effective nonlinear controller for an air-breathing engine. This control design approach does not normally require the tedious process of gain scheduling, even though that possibility is not ruled out. Here, all the states are not directly measurable. Hence, there is a need to estimate the states and to filter out the process and sensor noises. To meet these requirements, an Extended Kalman Filter based state estimation design has been carried out in parallel to augment the proposed control design. Note that the estimated states were used in the control design (in place of the actual states), which was passed through the actuator dynamics to test the performance of the controller. To avoid performance degradation due to slower actuators (as compared to the faster system dynamics), however, separate actuator controllers were also designed based on the dynamic inversion philosophy. The results obtained suggest that the control allocation strategy is a good one and both the control objectives are met successfully.

VII. ACKNOWLEDGMENTS

This research was supported by Coral Digital Technilogies (CDT), Bangalore, India with grant no. CP5755/0501/07. Fruitful technical discussions with Dr. N. Ananthkrishanan, Mr. B. Chandra, Mr. N. Gupta and Mr. V. S. Renganathan are gratefully acknowledged.

REFERENCES

[1] N. K. Gupta, B. K. Gupta, N. Ananthkrishnan, G. R. Shevare, I. S. Park and H. G. Yoon, "Integrated Modeling and Simulation of an Air-breathing Combustion System Dynamics", *AIAA Modeling and Simulation Technologies Conference and Exhibit*, AIAA Paper 2007-6374, 20-23 August, 2007, Hilton Head, South Carolina, USA

[2] P. B. Chandra, N. Gupta, N. Ananthkrishnan and V. Renganathan, I. Park and H. Yoon, "Modeling, Dynamic Simulation, and Controller Design for an Air-Breathing Combustion System", *47th AIAA Aerospace Sciences Meeting*, Paper Number: AIAA-2009-708, 5 - 8 January, 2009, Orlando, Florida.

[3] D. Enns, D. Bugajski, R. Hendrick and G. Stein, "Dynamic Inversion: An Evolving Methodology for Flight Control Design", *International Journal of Control*, vol. 59, no.1, 1994, pp 71-91.

[4] John L. Crassidis and John L. Junkins, *Optimal Estimation of Dynamic Systems*, chapter 5, CRC Press LLC, Florida, 2004.

[5] Mathworld,*http://mathworld.wolfram.com/DelaunayTriangulation.html*, Accessed on September 10, 2008.

[6] M. Fleifil, A. M. Annaswamy, J. P. Hathout and A. F. Ghoniem, "Reduced-Order Dynamic Models for Control of Reactive Fluid-flows," *Proceedings of the 38-th Conference on Decision & Control*, Phoenix, AZ, December, 1999, pp 2857-2862.

[7] J. Y. Oh, F. Ma, S. Y. Hsieh and V. Yang, "Interactions between Shock and AcousticWaves in a Supersonic Inlet Diffuser", *Journal of Propulsion and Power*, vol. 21, no. 3, May-June, 2005, pp 486-495.

[8] B. L. Stevens and F. L. Lewis, *Aircraft Control and Simulation*, Wiley, 1992.

[9] P. R. N. Childs, J. R. Greenwood and C. A. Long, *Review of temperature measurement*, Thermo-Fluid Mechanics Research Centre, University of Sussex, Brighton, United Kingdom, Received 22 July, 1999; accepted for publication 10th May, 2000.